Growth of Wetting Layers from Liquid Mixtures

Ullrich Steiner* and Jacob Klein

Department of Materials and Interfaces, Weizmann Institute of Science, Rehovot 76100, Israel

(Received 29 January 1996)

We have examined the growth with time t of the thickness l of wetting layers from thin films of binary fluid mixtures, using real-space composition-depth profiling based on nuclear reaction analysis. We find over a wide range of parameters that the observed growth behavior has a power law form $l \propto t^{\kappa}$, where κ is the range 0.2–0.3. Comparison with the predictions of a diffusion-limited wetting model shows that growth of the wetting layers is driven primarily by long-ranged surface fields. [S0031-9007(96)01138-6]

PACS numbers: 68.45.Gd, 68.10.Jy, 68.15.+e, 82.65.Dp

The evolution of wetting layers at the surface of mixtures of coexisting fluids—for example, a liquid and its vapor, or a mixture of two liquid phases—has important practical implications [1], but its understanding presents a considerable challenge. The growth of wetting layers from liquid mixtures, examined both experimentally and theoretically in several recent studies [2–15], is often convoluted by the presence of convective and gravitational fields, and of surface-directed spinodal decomposition. Here we report the evolution of wetting with time in a model binary fluid mixture where the wetting dynamics are strictly diffusion limited. This enables us to identify the nature of the surface fields driving the growth of the wetting layer.

Earlier studies demonstrated that complete wetting can occur in equilibrium from binary mixtures of random olefinic copolymer fluids [6,10] over a wide range of temperatures $T_w < T < T_c$. In the present work we examine in detail the *growth with time* of the wetting layers from two such mixtures. Each mixture is comprised of a pair of copolymers (kindly donated by Dr. L. J. Fetters), each of structure $([C_4H_8]_{1-x}\text{-}[C_2H_3\text{-}(C_2H_5)]_x)_N$, with different x values, where the ethyl ($[C_4H_8]$) and the ethylethlene ($[C_2H_3\text{-}(C_2H_5)]$) monomers are distributed randomly on the chains. N are the degrees of polymerization of the copolymers. Within each pair, the higher-x component is partially deuterated (and labeled dx_j, with x in %; the other—fully hydrogenated—component is labeled hx_i) to enable composition depth profiling by nuclear reaction analysis. The molecular characteristics are given in Table I. In each of the two couples the component with the higher branching ratio (higher x value) is the one preferred at the liquid/air interface [6,10].

Bilayers of the two components of each of the mixtures detailed in Table I—$h52/d66$ and $h78/d88$—were created by spin casting from analytical grade toluene solution. A uniform film of dx_j was spin cast on top of a gold covered silicon wafer, and a second film, of hx_i, was similarly cast on top of freshly cleaved mica, floated and mounted on top of the dx_j film. Bilayers were annealed in a vacuum oven ($<10^{-2}$ Torr) at temperatures T (stable to ± 0.3 °C) for different times t, following which they were stored at -80 °C (below the glass transition temperatures of all samples) prior to depth profiling. Each sample was used for a single annealing time. Depth vs concentration profiles of the deuterated species dx_j normal to the film surface were determined by nuclear reaction analysis (NRA) with a depth resolution of ca. 10 nm, as described earlier [16].

Figure 1 shows typical composition-depth profiles for $h52/d66$ bilayers, at an annealing temperature $T = 110$ °C. After an annealing time $t = 18$ h [Fig. 1(a)], the two layers of the pure $h52$ and $d66$ components have partially interdiffused, to establish the two coexisting phases at volume fractions ϕ_1 and ϕ_2 of the $d66$ component, $\phi_1 \approx 0.75$ and $\phi_2 \approx 0.25$. At the same time, a narrow surface peak of the $d66$ rich phase has evolved at the liquid-air interface [17]. The width l of the surface layer, indicated in Fig. 1, increases with annealing time, as seen in Fig. 1(b) ($t = 190$ h) and Fig. 1(c) ($t = 720$ h), with the plateau composition of the $d66$ surface layer at $\phi_1 \approx \phi_2$. The growth of this surface layer to macroscopic thickness (i.e., much larger than any microscopic correlation length in the mixtures), fully excluding the adjacent nonwetting phase, reveals directly the complete wetting of the free surface by the $d66$-rich phase. We should stress that gravitational potentials are negligible for the film thickness used, while the highly

TABLE I. Molecular characteristics of the $[(C_2H_3(C_2H_5))_x\text{-}(C_4H_8)_{1-x}]_N$ statistical copolymers, where x is the ethylethylene content, N the degree of polymerization, and f_D the fractional deuteration. Glass transition temperatures of all components lie in the range -34 to -65 °C. The couples used in the experiments were $h78/d88$ (critical temperature $T_C = 127$ °C [23]) and $h52/d66$ ($T_c = 204$ °C [23]).

Sample	x	N	f_D
$d88$	0.88	1610	0.34
$h78$	0.78	1290	
$d66$	0.66	2030	0.40
$h52$	0.52	1510	

 0031-9007/96/77(12)/2526(4)$10.00

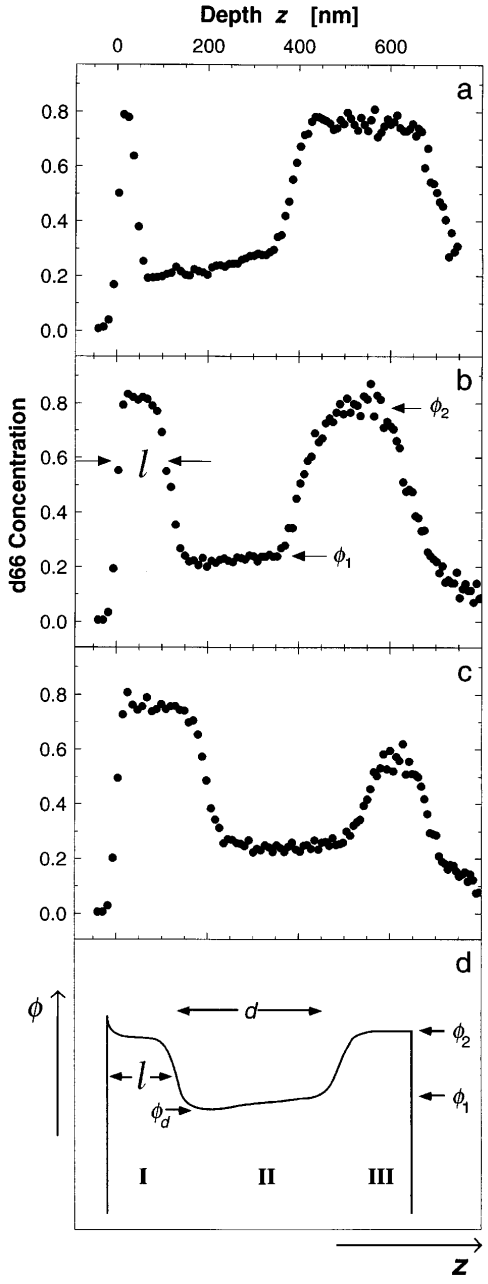

FIG. 1. Concentration-depth profiles for the $d66/h52$ mixture, annealed at 110 °C, determined by nuclear reaction analysis, (a) after 18 h, (b) after 190 h, and (c) after 720 h. The schematic drawing in (d) refers to the model presented in the text. The measured thickness of the wetting layer l is indicated in (b) as well as in the schematic of (d).

entangled nature of the polymers precludes convection effects in these measurements. The evolution of this wetting layer in the configuration of our experiments is analyzed below.

Figure 1(d) illustrates schematically the growth of the wetting layer in contact with the bulk of the sample following the transient initial stages [as in Fig. 1(a), during which interdiffusion to the coexisting compositions, and initial buildup of the surface layer occurs]. The depth-composition profile may be divided into three regions: (I) The wetting layer of thickness l and plateau composition $\phi_l \approx \phi_2$; (II) the nonwetting phase adjacent to I, of width d and a composition ϕ which varies between ϕ_d and ϕ_1; and (III) the "reservoir" phase of composition ϕ_2.

In our model we assume the wetting layer (region I) to be in local equilibrium with the immediately adjacent region of composition ϕ_d. When the wetting layer appears at the free surface, it depletes this adjacent region resulting in a concentration gradient in region II. Further growth of the wetting layer I [of thickness $l(t)$ and composition ϕ_l] is then fed by diffusion of the surface-preferred component from the nonwetting phase in region II. The growth of the wetting layer equals the flux of the surface-preferred phase through region II by diffusion from the reservoir phase" (region III) towards the surface. Excluding the initial stages, we have $\phi_l \approx \phi_2$ and $\phi_d \approx \phi_1$, while d stays constant with increasing annealing time, as seen clearly also from the profiles. Conservation of material then imposes

$$\frac{d}{dt}\{(\phi_2 - \phi_1)[l(t) - l(0)]\} = \frac{D(\phi_1, T)}{d}(\phi_1 - \phi_d), \tag{1}$$

where $D(\phi, T)$ is the concentration-dependent mutual diffusion coefficient [18–20]. To eliminate ϕ_d from Eq. (1), we express $\phi_1 - \phi_d$ in terms of the relative chemical potential [12],

$$\phi_1 - \phi_d = [\mu(\phi_1, T) - \mu(\phi_d, T)]\left(\frac{\partial \mu}{\partial \phi}\right)^{-1}_{\phi=\phi_1}. \tag{2}$$

Following Ref. [11] the chemical potential difference can be related to the interfacial potential $V(l)$,

$$\rho(\phi_2 - \phi_1)[\mu(\phi_1, T) - \mu(\phi_d, T)] = -\frac{\partial V}{\partial l}, \tag{3}$$

where $\rho = 1/a^3$ is the number density of monomers (a is the monomer or statistical segment size). Equations (1)–(3) are readily combined to solve for $l(t)$, where the chemical potentials are evaluated from the standard Flory-Huggins energy functional for polymer mixing [21]. This yields a differential equation which describes the growth with time of the wetting layer as a function of the derivative of the surface potential,

$$\frac{dl}{dt} = -\frac{\Omega_{\text{eff}}}{\rho d}\frac{\partial V(l)}{\partial l}. \tag{4}$$

Here $\Omega_{\text{eff}} = D_{\text{eff}}/k_B T$ is an effective mobility (k_B is Boltzmann's constant), where D_{eff} is an effective diffusion coefficient related directly to the mutual diffusion coefficient $D(\phi, T)$ [18].

We consider three different forms for $V(l)$. A short range attraction: $V(l) = -(A_s/a^2)\exp(-l/\zeta)$, where A_s is a surface potential term [22] and the decay length

$\zeta \approx a$; nonretarded van der Waals interactions (vdW): $V(l) = -A_{\rm nr}/12\pi l^2$, where $A_{\rm nr}$ is the nonretarded Hamaker constant, or retarded vdW, in the form $V(l) = -aA_r/l^3$, where A_r has units of energy and is an effective retarded Hamaker constant. Substitution in Eq. (4) yields the following relations:

$$\frac{l(t)}{\zeta} = \ln\left(\frac{-A_s a \Omega_{\rm eff} t}{d\zeta^2}\right) \quad \text{(short ranged)}, \tag{5a}$$

$$\frac{l(t)}{a} = \left(\frac{-2A_{\rm nr}}{3\pi}\,\frac{\Omega_{\rm eff} t}{da}\right)^{1/4} \quad \text{(nonretarded vdW)}, \tag{5b}$$

$$\frac{l(t)}{a} = \left(\frac{-A_r}{15}\,\frac{\Omega_{\rm eff} t}{da}\right)^{1/5} \quad \text{(retarded vdW)}. \tag{5c}$$

This analysis for diffusion-limited wetting from finite-sized mixtures follows the treatment by Lipowsky and Huse (LH) for wetting from a semi-infinite phase [12], but the predictions of Eq. (5) differ from theirs. The reason is that in finite-sized systems the conservation relation, Eq. (1), differs from that for semi-infinite systems treated by LH [12]. In particular, while their logarithmic prediction for short-ranged forces is qualitatively similar to Eq. (5a), LH predict a power-law dependence for wetting driven by retarded and nonretarded vdW forces with exponents $\frac{1}{8}$ and $\frac{1}{10}$, that is, one half those appearing in Eqs. (5b) and (5c), respectively.

Equation (5) shows that we may rescale our data in reduced coordinates: $l \to l/a$ and $t \to \Omega_{\rm eff} t/ad$. Use of these rescaled coordinates then enables us to superimpose, where necessary, data sets of different sample geometry (i.e., different d) and temperatures. Figure 2(a) shows the variation of the wetting layer thickness l versus the reduced time t/d on a log-log scale, for the $d88/h78$ couple. Here all annealing runs were carried out at $T = 110\,^{\circ}$C: Values of D were thus constant, and only the value of d varied, in the range from 270 to 530 nm. The data of Fig. 2(a) fits rather well to a power-law relation (solid line): $l \sim (t/d)^{\kappa}$, with $\kappa = 0.20 \pm 0.05$: This is close to the prediction of Eqs. (5b) or (5c); however, within the limited range of t/d, a logarithmic growth dependence of l [Eq. (5a)] describes the data equally well, as shown in the inset.

Figure 2(b) shows the variation of the wetting layer thickness l with time t for the $h52/d66$ mixture, from a large number of experiments at different annealing temperatures as well as different d values. The variation using the directly measured values of l and t is shown in the inset to Fig. 2, and reveals the large scatter of the data even within the double-logarithmic plot. In order to rescale the coordinates in terms of reduced layer thickness (l/a) and reduced time $(\Omega_{\rm eff} t/ad)$ according to Eq. (5), we use independently determined values of the coexisting compositions [23] ϕ_1, ϕ_2, and of $\Omega_{\rm eff}$ (via the directly determined self-diffusion coefficients) for the different copolymers [24]. The plot [main Fig. 2(b)] of the reduced wetting layer thickness l/a versus reduced time $D_{\rm eff} t/da$ reveals strikingly the collapse of the data. A power-law relation $l/a = (D_{\rm eff} t/ad)^{\kappa}$ [solid line, Fig. 2(b)] is clearly indicated over nearly 4 decades in the reduced time [25]. The best fit exponent is given by $\kappa = 0.30 \pm 0.05$, which lies slightly above the values predicted by Eqs. (5b) and (5c). A small systematic discrepancy in κ may reside in uncertainties [23] in the values of ϕ_1, ϕ_2, and $\Omega_{\rm eff}$ [18,24] used in the coordinate reduction.

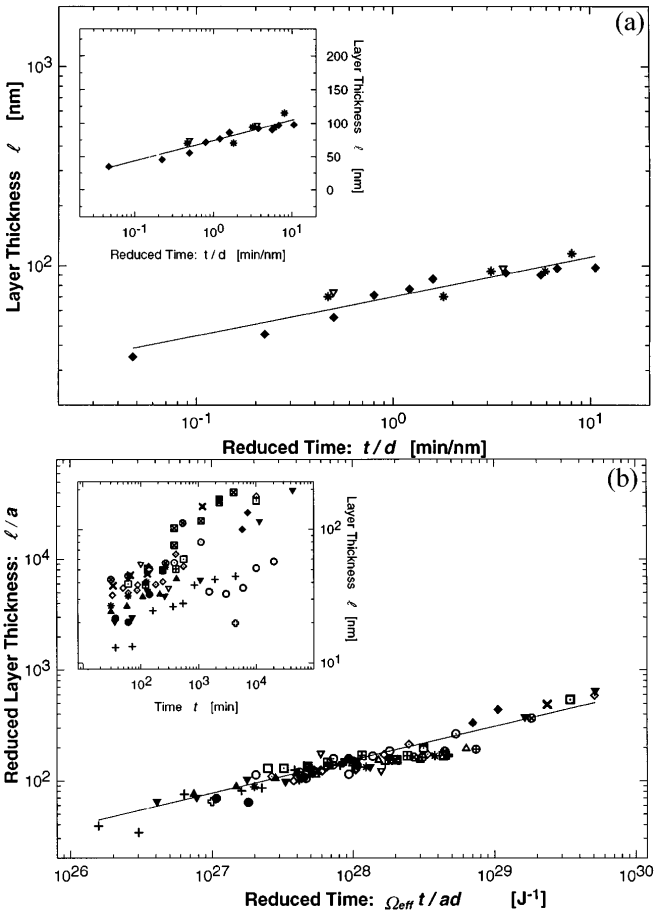

FIG. 2. (a) Wetting layer thickness l vs reduced time t/d for the $d88/h78$ couple annealed at 110 °C. The solid line is the relation $l \propto (t/d)^{0.20}$. The different symbols refer to varying values of d: *, $d = 315-530$ nm; ▽, $d = 360$ nm; ◆, $d = 270-340$ nm. (b) Variation of wetting layer thickness vs time for the $d66/h52$ couple. The inset shows the variation of the as-measured l with t, while the main figure plots the reduced thickness l/a vs reduced time $\Omega_{\rm eff} t/ad$. The solid line is the relation $l/a \propto (\Omega_{\rm eff} t/da)^{0.30}$. The different symbols designate varying temperatures and d spacings: ×, $T = 163\,^{\circ}$C, $d = 345$ nm; ✚, $T = 160\,^{\circ}$C, $d = 340$ nm; ⊗, $T = 154\,^{\circ}$C, $d = 215$ nm; ⊕, $T = 151\,^{\circ}$C, $d = 130$ nm; ⊞, $T = 150\,^{\circ}$C, $d = 590-670$ nm; ◇, $T = 150\,^{\circ}$C, $d = 500-680$ nm; ⊙, $T = 150\,^{\circ}$C, $d = 500-650$ nm; ⊡, $T = 150\,^{\circ}$C, $d = 545$ nm; ▽, $T = 150\,^{\circ}$C, $d = 510$ nm; ◇, $T = 150\,^{\circ}$C, $d = 310$ nm; △, $T = 150\,^{\circ}$C, $d = 250$ nm; □, $T = 149\,^{\circ}$C, $d = 325$ nm; *, $T = 140\,^{\circ}$C, $d = 120-250$ nm; ▼, $T = 110\,^{\circ}$C, $d = 335$ nm; ◆, $T = 110\,^{\circ}$C, $d = 315$ nm; ▲, $T = 110\,^{\circ}$C, $d = 175$ nm; ●, $T = 110\,^{\circ}$C, $d = 130$ nm; +, $T = 90\,^{\circ}$C, $d = 330$ nm; ○, $T = 70\,^{\circ}$C, $d = 275$ nm; ✣, $T = 45\,^{\circ}$C, $d = 260$ nm.

While the $l \propto t^{\kappa}$ power-law variation is suggestive, a *quantitative* comparison of Eq. (5) with the data is particularly revealing. Fitting the data of Figs. 2(a) and 2(b) to the nonretarded power law of Eq. (5b), using the Hamaker constant $A_{\rm nr}$ as a fit parameter, gives values $-A_{\rm nr}$ in the range $10^{-20}-10^{-21}$ J (within uncertainties resulting from scatter of the data). These are quantitatively reasonable values for these nonpolar liquids, and are fully consistent with the indication—from the power-law variation—that the wetting is driven by long-ranged fields. However, when we make a similar comparison with the prediction [Eq. (5a)] of short-range fields, a very different picture emerges. We find that despite the apparent fit to a logarithmic variation $l \propto \ln(t)$ [inset to Fig. 2(a)], the slope of the data, using the decay length ζ as a fit parameter, yields a value $\zeta \approx 31$ nm. Since short-range interactions must have a decay length ζ comparable with a monomer or statistical segment length $a \approx 6$ Å, Eq. (5a) cannot provide a consistent quantitative description of the $l(t)$ data [26]. We conclude that the growth of the wetting layer in these binary mixtures cannot be driven by short-ranged fields exclusively.

To summarize, we have investigated the growth with time of wetting layers from a binary fluid mixture, free of convective, gravitational, or spinodal demixing effects, using a direct depth profiling method. Quantitative comparison of our data with a diffusion-limited wetting model indicates that the surface fields driving the wetting cannot be exclusively short ranged. The time evolution of the wetting layer suggests that it is driven primarily by long-ranged van der Waals surface interactions.

We especially thank Lew Fetters for providing the polymers used in this work, David Andelman, Kurt Binder, Reinhard Lipowski, and Sam Safran for discussions, and a referee for a fruitful suggestion. Partial support from the German Israel Foundation, the Minerva Foundation, the Commission of the European Community, and the Ministry of Science and Arts (Israel) is gratefully acknowledged.

*Present address: Fakulttät für Physik, Universität Konstanz, D-78434 Konstanz, Germany

[1] For reviews see, for example, S. Dietrich, in *Phase Transitions and Critical Phenomena*, edited by C. Domb and J. L. Lebowitz (Academic, New York, 1988), Vol. XII, p. 1–218, especially 175 ff.; M. Schick, in *Liquids at Interfaces*, edited by J. Charvolin, J-F. Joanny, and J. Zinn-Justin (North-Holland, Amsterdam, 1990), pp. 419–497.

[2] R. F. Kayser, M. R. Moldover, and J. W. Schmidt, J. Chem. Soc. Faraday Trans. II **82**, 1701 (1986).

[3] X.-l. Wu, M. Schlossman, and C. Franck, Phys. Rev. B **33**, 402 (1986).

[4] P. Guenon and D. Beysens, Phys. Rev. Lett. **65**, 2406 (1990).

[5] P. Wiltzius and A. Cumming, Phys. Rev. Lett. **66**, 3000 (1991).

[6] U. Steiner, J. Klein, E. Eiser, A. Budkowski, and L. Fetters, Science **258**, 1126 (1992).

[7] F. Bruder and R. Brenn, Phys. Rev. Lett **69**, 624 (1992).

[8] B. Q. Shi, C. Harrison, and A. Cumming, Phys. Rev. Lett. **70**, 206 (1993).

[9] B. M. Law, Phys. Rev. Lett. **72**, 1698 (1994).

[10] U. Steiner, J. Klein, and L. J. Fetters, Phys. Rev. Lett. **72**, 1498 (1994).

[11] R. Lipowsky, Phys. Rev. B **32**, 1731 (1985).

[12] R. Lipowsky and D. A. Huse, Phys. Rev. Lett. **57**, 353 (1986).

[13] K. K. Mon, K. Binder, and D. P. Landau, Phys. Rev. B **35**, 3683 (1987).

[14] R. A. L. Jones, L. J. Norton, E. J. Kramer, F. Bates, and P. Wiltzius, Phys. Rev. Lett. **66**, 1326 (1991).

[15] G. Krausch, C.-A. Dai, E. J. Kramer, and F. S. Bates, Phys. Rev. Lett. **71**, 3669 (1993).

[16] J. Klein, Science **250**, 640 (1990); U. K. Chaturvedi, U. Steiner, O. Zak, G. Krausch, G. Schatz, and J. Klein, Appl. Phys. Lett. **56**, 1228 (1990).

[17] There is no evidence in any of our profiles (or in analogous studies [6,22,23]) for enrichment by either of the phases at the liquid-solid interface.

[18] $D_{\rm eff} = D(\phi,T)/\{2[\chi_s(\phi) - \chi](\phi_2 - \phi_1)^2\}$. The mutual diffusion coefficient is given by [19,20] $D(\phi,T) = 2\phi(1-\phi)[D_a^* N_a(1-\phi) + D_b^* N_b \phi][\chi_s(\phi) - \chi]$, where the value of the interaction parameter at the spinodal $\chi_s(\phi) = \{(N_a\phi)^{-1} + [N_b(1-\phi)]^{-1}\}/2$. Here N_a, N_b are the polymerization indices of the two polymers, and D_a^*, D_b^* their tracer diffusion coefficients (approximated for our polymers from their respective self-diffusion coefficients [24]).

[19] R. J. Composto, E. J. Kramer, and D. M. White, Nature (London) **328**, 234 (1987).

[20] A. Losch, D. Wörmann, and J. Klein, Macromolecules **27**, 5713 (1994).

[21] P. J. Flory, *Principles of Polymer Chemistry* (Cornell University Press, Ithaca, 1953).

[22] F. Scheffold, A. Budkowski, U. Steiner, E. Eiser, J. Klein, and L. J. Fetters, J. Chem. Phys. **104**, 8795 (1996).

[23] F. Scheffold, E. Eiser, A. Budkowski, U. Steiner, J. Klein, and L. J. Fetters, J. Chem. Phys. **104**, 8786 (1996).

[24] A. Losch, R. Salomonovic, U. Steiner, L. J. Fetters, and J. Klein, J. Polym. Sci., Polym. Phys. Ed. **33**, 1821 (1995).

[25] We note that for these data sets a log-linear plot (not shown) using the same reduced parameters shows a distinct curvature, suggesting that a logarithmic relation, as predicted in Eq. (5a) for short-ranged surface interactions, is not too well obeyed.

[26] For example, if we impose $\zeta = a$ in Eq. (5a), with a value $A_s = 0.02 k_B T$ estimated from equilibrium adsorption studies [22], we find a time of ca. 10^{60} yr required for the wetting layer to grow to 100 nm if driven by short-range forces alone.